Perfluoroalkane Functionalization of NU-1000 via Solvent-Assisted Ligand Incorporation: Synthesis and CO$_2$ Adsorption Studies

Pravas Deria,[†] Joseph E. Mondloch,[†] Emmanuel Tylianakis,[†,‡] Pritha Ghosh,[†] Wojciech Bury,[†,§] Randall Q. Snurr,*[,†] Joseph T. Hupp,*[,†] and Omar K. Farha*[,†]

[†]Departments of Chemistry and Chemical and Biological Engineering, Northwestern University, 2145 Sheridan Road, Evanston, Illinois 60208, United States

[‡]Materials Science and Technology Department, University of Crete, P.O. Box 2208, 71409 Heraklion, Crete, Greece

[§]Department of Chemistry, Warsaw University of Technology, Noakowskiego 3, 00-664 Warsaw, Poland

Ⓢ *Supporting Information*

ABSTRACT: A new functionalization technique, solvent-assisted ligand incorporation (SALI), was developed to efficiently incorporate carboxylate-based functionalities in the Zr-based metal−organic framework, **NU-1000**. Unlike previous metal node functionalization strategies, which utilize dative bonding to coordinatively unsaturated metal sites, SALI introduces functional groups as charge compensating and strongly bound moieties to the Zr$_6$ node. Utilizing SALI, we have efficiently attached perfluoroalkane carboxylates of various chain lengths (C$_1$−C$_9$) on the Zr$_6$ nodes of **NU-1000**. These fluoroalkane-functionalized mesoporous MOFs, termed herein **SALI-n**, were studied experimentally and theoretically as potential CO$_2$ capture materials.

Metal−organic frameworks (MOFs) constitute a rapidly growing class of solid-state compounds. They are built up from multitopic organic linkers and metal-based nodes which are interconnected by coordination bonds of moderate strength.[1] From a functional materials perspective, due to their chemical diversity and high surface area,[2] MOFs have garnered tremendous interest for many practical applications including gas storage and separation,[3] chemical catalysis,[4] sensing,[5] conductivity,[6] and light harvesting.[7] Given the highly modular nature of MOFs, the introduction of chemical functionality should be straightforward (at least in comparison to many other solid-state materials). Unfortunately, de novo syntheses (i.e., one-pot solvothermal syntheses) often encounter problems associated with linker solubility, linker stability, and/or the formation of undesirable structures or side products (e.g., the coordination of metal ions to the functionalized linker).[8]

Postsynthesis incorporation of desired functionality within a given MOF structure has proven to be a key strategy in overcoming many synthetic challenges associated with de novo MOF preparation.[8] Some of the most attractive strategies include functionalization at the metal node (via dative bonding),[9] covalent modification of the organic linker,[10] and solvent-assisted linker exchange (SALE)[11] which involves completely exchanging one organic linker for another. In the context of functional materials, MOFs with high chemical and thermal stability are desirable. Among the various metal-based

nodes, MOFs constructed from oxophilic Zr$^{IV}_6$ nodes have high thermal (up to 500 °C), chemical (pH 1−10),[12] and mechanical stability.[12,13] Recently, we[14] and others[15] have focused our attention on mesoporous Zr-based MOFs. **NU-1000** (Scheme 1) consists, in part, of an octahedral Zr$_6$ cluster

Scheme 1. (A) Molecular Representations of NU-1000 and (B) Schematic Representation of Solvent-Assisted Ligand Incorporation (SALI)
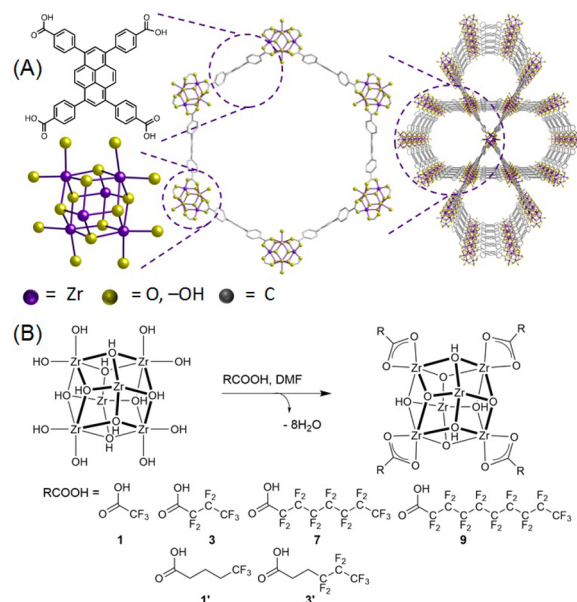
capped by eight μ_3-OH ligands.[16] Eight of the 12 octahedral edges are connected to TBAPy linkers (H$_4$TBAPy = 1,3,6,8-tetrakis(p-benzoic acid)pyrene), while the remaining Zr coordination sites are occupied by eight terminal −OH ligands. The resultant MOF has the molecular formula Zr$_6$(μ_3-OH)$_8$(−OH)$_8$(TBAPy)$_2$ and contains mesoporous channels lined with terminal −OH ligands[14] (∼20−25% of the mesoporous channels contain a secondary structural element;

Table 1. BET Surface Areas, Pore Diameters, Pore Volumes, CO_2 Uptake and Q_{st}^0 for SALI-n Samples, and NU-1000

MOF	ligand	ligand/ Zr_6[a]	BET surface area (m^2/g)	BJH pore diameter (Å)	pore volume[b] (cc/g)	CO_2 uptake @ 0.15 bar (cc/cc)[c]	Q_{st}^0 (kJ/mol)
NU-1000			2320	31	1.4	5.6	17
SALI-1	$CF_3CO_2^-$	4	1710	30	1	9.4	24
SALI-3	$CF_3(CF_2)_2CO_2^-$	3.8	1410	30	0.8	8.8	28
SALI-7	$CF_3(CF_2)_6CO_2^-$	3.7	900	28	0.6	7.2	31
SALI-9	$CF_3(CF_2)_8CO_2^-$	3.4	870	28	0.6	6.2	34
SALI-1′	$CF_3(CH_2)_3CO_2^-$	2	1600	30	1	6.4	21
SALI-3′	$CF_3(CF_2)_2(CH_2)_2CO_2^-$	3	1400	30	0.9	5.3	24

[a]See SI section S7. [b]See SI section S14. [c]T = 273 K.

see Supporting Information (SI) section S1D), which are attractive for introducing new functionality (vide infra).

In the context of carbon capture and sequestration (CCS),[17] fluorinated MOFs[18] have recently emerged as attractive candidates given their hydrophobicity and the presence of X−F dipoles (where, for example, X can be C,[18d,f] P,[18e] Si[18b,c]). Hydrophobicity should render the MOF stable toward water vapor,[18a] a component in postcombustion CO_2 capture, while the presence of C−F dipoles should lead to favorable interactions with the quadrupole of CO_2 (i.e., high isosteric heats of adsorption, Q_{st}).[18f,19] For example, Eddaoudi has shown an enhancement of CO_2 adsorption in MOFs containing C−F dipoles in the linker; Q_{st}^0 values as high as 60 kJ/mol[18f] have been observed. Likewise, MOFs constructed with pyrazine and bipyridine linkers that utilize anionic hexafluorophosphate[18e] and hexafluorosilicate[18b] as pillars have demonstrated high selectivity for CO_2 with moderate to high Q_{st}^0 values (31−45 kJ/mol).

However, to date, no study has systematically investigated the effects of alkyl C−F dipole[19c] on CO_2 adsorption. Hence we sought to utilize the $[Zr_6(\mu_3\text{-}OH)_8(-OH)_8]^{8+}$ node of NU-1000, functioning as a platform for solvent-assisted ligand incorporation (SALI), to introduce perfluoroalkane functionality within its mesoporous channels. Perfluoroalkyl carboxylic acids of varying chain length (1, 3, 7, and 9; Scheme 1) were utilized. Likewise fluoroalkanes bonded to the carboxylic acids via ethylene (CH_2−CH_2) and propylene (CH_2−CH_2−CH_2) moieties were utilized to better understand any cooperative CO_2 adsorption effects between the perfluoroalkanes and the Zr_6 node. Unlike previous metal node functionalization strategies, which utilize dative bonding to coordinatively unsaturated metal sites,[20] *SALI relies on acid−base chemistry between the hydroxyl groups on the NU-1000 node and the carboxylate group of the perfluorinated chain.* This results in the introduction of functional groups as charge compensating and strongly bound moieties to the NU-1000 node via ionic bonding. Furthermore, while the nodes of Zr-based MOFs have previously been functionalized with various metals,[14,21] to our knowledge, this is the first example utilizing the node to introduce carbon-based functionality.

To start, a microcrystalline powder of NU-1000 was synthesized as previously described[14] and exposed to a 0.1 M solution of fluoroalkyl carboxylic acid (i.e., 8 equiv per Zr_6 node) in DMF at 60 °C for 18−24 h (see SI for a detailed description). The degree of functionalization was quantified by ^{1}H and ^{19}F NMR after decomposing the samples in a 10% D_2SO_4/DMSO-d_6 mixture; the ^{19}F signals of the perfluoroalkanes (1, 3, 7, and 9; Scheme 1) were integrated against the ^{1}H NMR signals of the TBAPy ligand using an internal standard (2,5-dibromo-1,4-bis(trifluoromethyl)benzene; see SI

section S6). Approximately 3.4−4 perfluoroalkyl carboxylates, per Zr_6 node, can be incorporated within NU-1000 (Table 1). (Complete functionalization considering the SALI stoichiometry shown in Scheme 1 is four carboxylates per Zr_6 node; see SI section S7.) We have termed the resultant materials SALI-n (e.g., SALI-1−SALI-9), where n is the carboxylic acid ligand described in Scheme 1. To ensure the maximum accessibility of the Zr_6 node by these carboxylates, SALI experiments were carried out at higher temperature (80 °C) and longer times (36 h). The degree of functionalization for these extended exposures was the same as those at lower temperature and shorter time (i.e., ~4 fluorocarboxylates per Zr_6 cluster).

Powder X-ray diffraction (PXRD) measurements (Figure 1A and Figure SI-6) confirmed that the functionalized samples
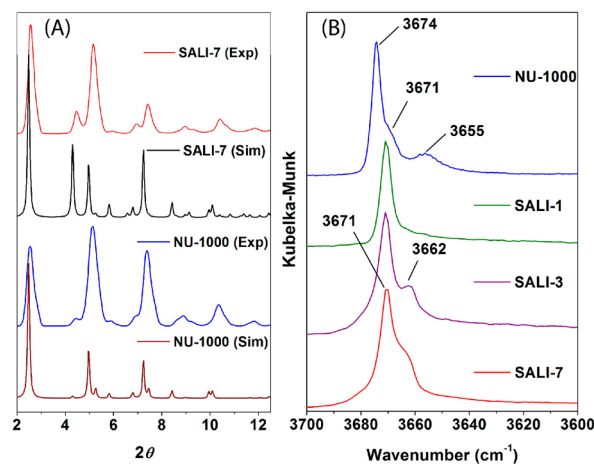

Figure 1. (A) PXRD patterns of NU-1000 simulated (Sim), NU-1000 experimental (Exp), SALI-7 simulated (Sim) from the model structure and SALI-7 (Exp). (B) DRIFTS spectra for NU-1000, SALI-1, SALI-3, and SALI-7.

retain their crystallinity. Note the change in relative intensities of the peaks that appear at 2θ values of 2.5, 4.5, and 5 upon functionalization. Going from a shorter to longer alkyl chain (e.g., SALI-1 to SALI-9), the intensity of the peak at 2θ = 4.5 increases; this change is similar to those observed previously for samples of NU-1000 metalated at the node.[14] The results can be explained by functionalization occurring at the $[Zr_6(\mu_3\text{-}OH)_8(-OH)]^{8+}$ node of NU-1000 (i.e., increased electron density about the 010 plane where a significant portion of the Zr_6 node is sited).

Further evidence consistent with functionalization at the node is provided by the results of diffuse reflectance infrared Fourier transform spectroscopy (DRIFTS) measurements. A peak appears at 3674 cm^{-1} which we assign to terminal −OH

groups, while a shoulder at 3671 cm^{-1} is consistent with the bridging μ_3-OH groups observed for **UiO-66**.[22] For **SALI-1**, **SALI-3**, and **SALI-7** (Figure 1B), clear disappearance of the sharp peak at 3674 cm^{-1} indicates that only the terminal −OH sites are occupied by the fluoroalkyl carboxylates in these functionalized samples, where the peak for the remaining bridging −OH ligands can be discerned at 3671 cm^{-1} (also see Figure SI-3). Given that functionalization on the Zr$_6$ node by four carboxylates causes spectral disappearance of all eight terminal −OH ligands, we postulate that the local coordination environment of the nodes of **SALI-n** functionalization is similar to that of **UiO-66** (Figure 1B). Thus, the added carboxylate ligands in **SALI-n** compounds coordinate to each of the four equatorial Zr^{IV} ions as bidentate ligands, with a resultant molecular formula Zr$_6(\mu_3$-O)$_4(\mu_3$-OH)$_4$(CO$_2^-$)$_{12}$ (Figure SI-4). Functionalization of **NU-1000** with four fluoroalkyl carboxylates involves net removal of eight water molecules (Scheme 1). Notably, the DRIFTS spectrum of **SALI-1** in Figure 1B is identical to that of the as-synthesized form of **NU-1000**,[14] where, in addition to linkers, the Zr$_6$ cluster of this form features four chelating benzoates (residual modulators).

The N$_2$ adsorption isotherms of the fluoroalkane-functionalized **SALI-n** samples retain the type IVc shape found for the parent **NU-1000**. Brunauer−Emmett−Teller (BET) analyses of the isotherms (Figure 2A) indicate a systematic decrease in
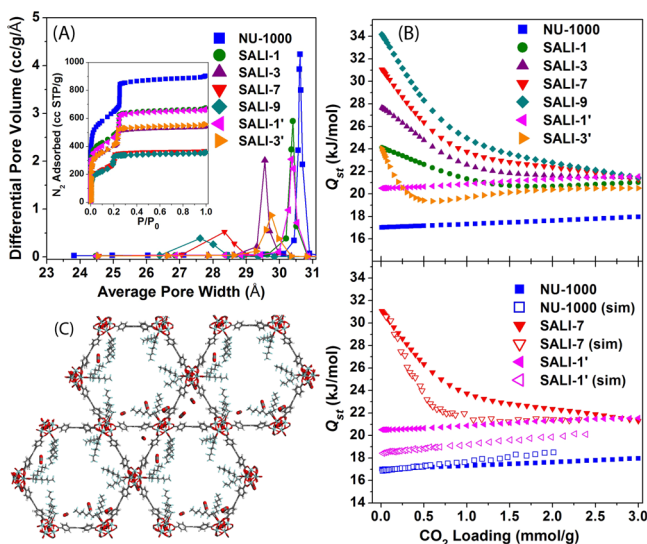
higher volumetric uptake (Table 1) at low-pressure (∼0.15 bar).

In order to estimate the average binding energy of CO$_2$ to the perfluoroalkane-modified samples, we analyzed isotherms collected at different temperatures. Briefly, single-site or dual-site Langmuir models followed by Clausius−Clapeyron analysis were utilized to extract loading-dependent values of Q_{st} for each compound (Figure 2B and Table 1 and SI). In the zero-uptake limit (Q_{st}^0), all **SALI-n** samples showed a higher value than unmodified **NU-1000**, with the value systematically increasing with fluoroalkane chain length. The value of Q_{st}^0 for **SALI-9** is twice that for unmodified **NU-1000**.[23] The Q_{st} plots for all **SALI-n** samples show a decrease to ∼21 kJ/mol, which corresponds to the heat of adsorption for the weaker binding sites at higher CO$_2$ loading. For **SALI-1** and **SALI-9**, the Q_{st} plateaus at a loading of 1.5 and 1.0 mmol/g of MOF, respectively; these correspond to ∼1 CO$_2$ per fluoroalkane chain. These findings are consistent with pore confinement playing a crucial role in CO$_2$−sorbent interaction similar to the observations reported by Eddaoudi[18f] and Zhou.[24] Note that the Q_{st} values for the **SALI-n** samples are higher than the enthalpy of liquefaction for CO$_2$ (17 kJ/mol) and similar to the Q_{st} for MOFs with open metal sites such as **Co-MOF-74**[25] and **HKUST-1**.[26] To detect possible synergistic effects due to the zirconium-oxo node contributing to the CF−CO$_2$ interaction, we studied **SALI-1′** and **SALI-3′**. Here the fluoroalkane chains are bonded to the carboxylate functionality via an ethylene or propylene moiety (Scheme 1). The Q_{st}^0 values for both of these **SALI-n′** samples are ∼3−4 kJ/mol lower than their corresponding perfluoroalkyl counterparts. Additionally, the Q_{st} plot of **SALI-1′**, as a function of CO$_2$ loading, is similar to that of the unmodified **NU-1000** sample, with the exception of slightly higher Q_{st}. These results are in agreement with a recent study reporting synergistic (additive) Q_{st} effects of polar hexaterbium and hexayttrium nodes for CO$_2$ adsorption within MOFs.[18f]

Theoretical modeling confirmed our experimental observations: (1) the simulated Q_{st} (Figure 2B, bottom) for respective model MOFs are in good agreement with the experimental data and (2) primary CO$_2$ binding sites are close to the Zr$_6$ nodes (Figure 2C and Figure SI-19). Though the ideal adsorbed solution theory (IAST)[27] calculated selectivity for the CO$_2$ adsorption over N$_2$ (CO$_2$/N$_2$ = 10:90) was low in these mesoporous MOF structures (see S18), preference for CO$_2$ adsorption increases in the long perfluoroalkyl-functionalized **SALI-9** compared to the nonfunctionalized **NU-1000**. Water adsorption data indicate only modest enhancement in hydrophobicity upon perfluoroalkane functionalization (see S19).

In conclusion, we have developed an efficient functionalization method for Zr-based mesoporous MOFs based on solvent-assisted ligand incorporation. Spectroscopic data indicate that these carboxylates are bound to the Zr$_6$ node, likely resulting in a **UiO-66**-type metal node, Zr$_6(\mu_3$-OH)$_4(\mu_3$-O)$_4$(CO$_2^-$)$_{12}$. CO$_2$ adsorption studies indicate that perfluoroalkane-functionalized nodes in the **SALI-n** system synergistically act as the primary CO$_2$ binding sites manifesting in systematically higher values for Q_{st} with increasing chain length. We anticipate that SALI will prove attractive for enhancing chemical competency and functionality within MOFs for a wide variety of applications, including catalysis, sorption, and separations.

Figure 2. (A) BJH pore size distributions and N$_2$ adsorption isotherms (inset) for **NU-1000** and **SALI-n** samples. (B) Q_{st} of **NU-1000**, **SALI-n** and **SALI-n′** samples: (top) calculated from experimental isotherm data and (bottom) comparison of simulated (sim) and experimental Q_{st} values for selected MOFs. (C) Simulated snapshot of CO$_2$ adsorption depicting the primary CO$_2$ binding sites in **SALI-7** (T = 293 K and P = 0.1 bar).

surface area from 2320 m^2 g^{-1} for **NU-1000** to 1710 and 870 for **SALI-1** and **SALI-9**. As expected, the gravimetric and volumetric surface areas, along with pore sizes and pore volumes, decrease as a function of chain length. The CO$_2$ adsorption isotherm for **NU-1000** shows Langmuir-type behavior with an uptake of 31 cc/cc at 1 bar (T = 273 K; Figures SI-11 and SI-12). In contrast, the CO$_2$ adsorption profiles (Figures SI-11 and SI-12) for all the **SALI-n** derivatives show a steeper uptake in the isotherm resulting, in general,

ASSOCIATED CONTENT

S Supporting Information

Procedure, characterization, structure modeling, CO_2 and water sorption data. This material is available free of charge via the Internet at http://pubs.acs.org.

AUTHOR INFORMATION

Corresponding Author

snurr@northwestern.edu; j-hupp@northwestern.edu; o-farha@northwestern.edu

Notes

The authors declare no competing financial interest.

ACKNOWLEDGMENTS

REFERENCES

(1) (a) Yaghi, O. M.; O'Keefe, M.; Ockwig, N. W.; Chae, H. K.; Eddaoudi, M.; Kim, J. *Nature* **2003**, *423*, 705. (b) Férey, G. *Chem. Soc. Rev.* **2008**, *37*, 191. (c) Horike, S.; Shimomura, S.; Kitagawa, S. *Nat. Chem.* **2009**, *1*, 695.

(2) Farha, O. K.; Eryazici, I.; Jeong, N. C.; Hauser, B. G.; Wilmer, C. E.; Sarjeant, A. A.; Snurr, R. Q.; Nguyen, S. T.; Yazaydın, A. Ö.; Hupp, J. T. *J. Am. Chem. Soc.* **2012**, *134*, 15016.

(3) (a) Farha, O. K.; Yazaydın, A. Ö.; Eryazici, I.; Malliakas, C. D.; Hauser, B. G.; Kanatzidis, M. G.; Nguyen, S. T.; Snurr, R. Q.; Hupp, J. T. *Nat. Chem.* **2010**, *2*, 944. (b) Zhou, H.-C.; Long, J. R.; Yaghi, O. M. *Chem. Rev.* **2012**, *112*, 673.

(4) (a) Ma, L.; Abney, C.; Lin, W. *Chem. Soc. Rev.* **2009**, *38*, 1248. (b) Lee, J.; Farha, O. K.; Roberts, J.; Scheidt, K. A.; Nguyen, S. T.; Hupp, J. T. *Chem. Soc. Rev.* **2009**, *38*, 1450.

(5) Kreno, L. E.; Leong, K.; Farha, O. K.; Allendorf, M.; Van Duyne, R. P.; Hupp, J. T. *Chem. Rev.* **2012**, *112*, 1105.

(6) (a) Sun, L.; Miyakai, T.; Seki, S.; Dincă, M. *J. Am. Chem. Soc.* **2013**, *135*, 8185. (b) Jeong, N. C.; Samanta, B.; Lee, C. Y.; Farha, O. K.; Hupp, J. T. *J. Am. Chem. Soc.* **2012**, *134*, 51. (c) Horike, S.; Umeyama, D.; Kitagawa, S. *Acc. Chem. Res.* **2013**, DOI: 10.1021/ar300291s.

(7) (a) Jin, S.; Son, H.-J.; Farha, O. K.; Wiederrecht, G. P.; Hupp, J. T. *J. Am. Chem. Soc.* **2013**, *135*, 955. (b) Son, H.-J.; Jin, S.; Patwardhan, S.; Wezenberg, S. J.; Jeong, N. C.; So, M.; Wilmer, C. E.; Sarjeant, A. A.; Schatz, G. C.; Snurr, R. Q.; Farha, O. K.; Wiederrecht, G. P.; Hupp, J. T. *J. Am. Chem. Soc.* **2013**, *135*, 862. (c) Kent, C. A.; Mehl, B. P.; Ma, L.; Papanikolas, J. M.; Meyer, T. J.; Lin, W. *J. Am. Chem. Soc.* **2010**, *132*, 12767.

(8) Cohen, S. M. *Chem. Rev.* **2012**, *112*, 970.

(9) (a) Hwang, Y. K.; Hong, D.-Y.; Chang, J.-S.; Jhung, S. H.; Seo, Y.-K.; Kim, J.; Vimont, A.; Daturi, M.; Serre, C.; Férey, G. *Angew. Chem., Int. Ed.* **2008**, *47*, 4144. (b) Farha, O. K.; Mulfort, K. L.; Hupp, J. T. *Inorg. Chem.* **2008**, *47*, 10223. (c) Seo, J. S.; Whang, D.; Lee, H.; Jun, S. I.; Oh, J.; Jeon, Y. J.; Kim, K. *Nature* **2000**, *404*, 982.

(10) Kiang, Y.-H.; Gardner, G. B.; Lee, S.; Xu, Z.; Lobkovsky, E. B. *J. Am. Chem. Soc.* **1999**, *121*, 8204.

(11) (a) Bury, W.; Fairen-Jimenez, D.; Lalonde, M. B.; Snurr, R. Q.; Farha, O. K.; Hupp, J. T. *Chem. Mater.* **2013**, *25*, 739. (b) Karagiaridi, O.; Bury, W.; Sarjeant, A. A.; Stern, C. L.; Farha, O. K.; Hupp, J. T. *Chem. Sci.* **2012**, *3*, 3256. (c) Karagiaridi, O.; Lalonde, M. B.; Bury, W.; Sarjeant, A. A.; Farha, O. K.; Hupp, J. T. *J. Am. Chem. Soc.* **2012**, *134*,

18790. (d) Takaishi, S.; DeMarco, E. J.; Pellin, M. J.; Farha, O. K.; Hupp, J. T. *Chem. Sci.* **2013**, *4*, 1509. (e) Li, T.; Kozlowski, M. T.; Doud, E. A.; Blakely, M. N.; Rosi, N. L. *J. Am. Chem. Soc.* **2013**, *135*, 11688. (f) Kim, M.; Cahill, J. F.; Su, Y.; Prather, K. A.; Cohen, S. M. *Chem. Sci.* **2012**, *3*, 126. (g) Burnett, B. J.; Barron, P. M.; Hu, C.; Choe, W. *J. Am. Chem. Soc.* **2011**, *133*, 9984.

(12) Cavka, J. H.; Jakobsen, S.; Olsbye, U.; Guillou, N.; Lamberti, C.; Bordiga, S.; Lillerud, K. P. *J. Am. Chem. Soc.* **2008**, *130*, 13850.

(13) Wu, H.; Yildirim, T.; Zhou, W. *J. Phys. Chem. Lett.* **2013**, *4*, 925.

(14) Mondloch, J. E.; Bury, W.; Fairen-Jimenez, D.; Kwon, S.; DeMarco, E. J.; Weston, M. H.; Sarjeant, A. A.; Nguyen, S. T.; Stair, P. C.; Snurr, R. Q.; Farha, O. K.; Hupp, J. T. *J. Am. Chem. Soc.* **2013**, *135*, 10294.

(15) (a) Morris, W.; Volosskiy, B.; Demir, S.; Gándara, F.; McGrier, P. L.; Furukawa, H.; Cascio, D.; Stoddart, J. F.; Yaghi, O. M. *Inorg. Chem.* **2012**, *51*, 6443. (b) Feng, D.; Gu, Z.-Y.; Li, J.-R.; Jiang, H.-L.; Wei, Z.; Zhou, H.-C. *Angew. Chem., Int. Ed.* **2012**, *51*, 10307. (c) Chen, Y.; Hoang, T.; Ma, S. *Inorg. Chem.* **2012**, *51*, 12600.

(16) An alternative formulation of the **NU-1000** structure would feature oxo and aquo ligands in place of hydroxo ligands. Either formulation can yield the subsequently observed ligand incorporation chemistry. For simplicity, we will henceforth refer only to the hydroxo alternative.

(17) (a) Li, J.-R.; Sculley, J.; Zhou, H.-C. *Chem. Rev.* **2012**, *112*, 869. (b) Sumida, K.; Rogow, D. L.; Mason, J. A.; McDonald, T. M.; Bloch, E. D.; Herm, Z. R.; Bae, T.-H.; Long, J. R. *Chem. Rev.* **2012**, *112*, 724. (c) Liu, J.; Thallapally, P. K.; McGrail, B. P.; Brown, D. R.; Liu, J. *Chem. Soc. Rev.* **2012**, *41*, 2308.

(18) (a) Yang, C.; Kaipa, U.; Mather, Q. Z.; Wang, X.; Nesterov, V.; Venero, A. F.; Omary, M. A. *J. Am. Chem. Soc.* **2011**, *133*, 18094. (b) Nugent, P.; Belmabkhout, Y.; Burd, S. D.; Cairns, A. J.; Luebke, R.; Forrest, K.; Pham, T.; Ma, S.; Space, B.; Wojtas, L.; Eddaoudi, M.; Zaworotko, M. J. *Nature* **2013**, *495*, 80. (c) Kanoo, P.; Reddy, S. K.; Kumari, G.; Haldar, R.; Narayana, C.; Balasubramanian, S.; Maji, T. K. *Chem. Commun.* **2012**, *48*, 8487. (d) Wilmer, C. E.; Farha, O. K.; Bae, Y.-S.; Hupp, J. T.; Snurr, R. Q. *Energy Environ. Sci.* **2012**, *5*, 9849. (e) Noro, S.-i.; Hijikata, Y.; Inukai, M.; Fukushima, T.; Horike, S.; Higuchi, M.; Kitagawa, S.; Akutagawa, T.; Nakamura, T. *Inorg. Chem.* **2013**, *52*, 280. (f) Xue, D.-X.; Cairns, A. J.; Belmabkhout, Y.; Wojtas, L.; Liu, Y.; Alkordi, M. H.; Eddaoudi, M. *J. Am. Chem. Soc.* **2013**, *135*, 7660. (g) Fernandez, C. A.; Thallapally, P. K.; Motkuri, R. K.; Nune, S. K.; Sumrak, J. C.; Tian, J.; Liu, J. *Cryst. Growth Des.* **2010**, *10*, 1037.

(19) (a) DeSimone, J. M.; Maury, E. E.; Menceloglu, Y. Z.; McClain, J. B.; Romack, T. J.; Combes, J. R. *Science* **1994**, *265*, 356. (b) Fried, J. R.; Hu, N. *Polymer* **2003**, *44*, 4363. (c) Dalvi, V. H.; Srinivasan, V.; Rossky, P. J. *J. Phys. Chem. C* **2010**, *114*, 15553.

(20) (a) McDonald, T. M.; D'Alessandro, D. M.; Krishna, R.; Long, J. R. *Chem. Sci.* **2011**, *2*, 2022. (b) Zheng, S.-T.; Zhao, X.; Lau, S.; Fuhr, A.; Feng, P.; Bu, X. *J. Am. Chem. Soc.* **2013**, *135*, 10270.

(21) Larabi, C.; Quadrelli, E. A. *Eur. J. Inorg. Chem.* **2012**, *2012*, 3014.

(22) Valenzano, L.; Civalleri, B.; Chavan, S.; Bordiga, S.; Nilsen, M. H.; Jakobsen, S.; Lillerud, K. P.; Lamberti, C. *Chem. Mater.* **2011**, *23*, 1700.

(23) The observed large differences in Q_{st}^0 values for CO_2 uptake by various **SALI-n** materials versus **NU-1000** imply that affinity constants from fits of the corresponding CO_2 sorption isotherms should be 1 to 3 orders of magnitude larger for the **SALI-n** materials than for **NU-1000**. As shown in the SI, these expectations are indeed borne out.

(24) Li, J.-R.; Yu, J.; Lu, W.; Sun, L.-B.; Sculley, J.; Balbuena, P. B.; Zhou, H.-C. *Nat. Commun.* **2013**, *4*, 1538.

(25) Caskey, S. R.; Wong-Foy, A. G.; Matzger, A. J. *J. Am. Chem. Soc.* **2008**, *130*, 10870.

(26) Wang, Q. M.; Shen, D.; Bülow, M.; Lau, M. L.; Deng, S.; Fitch, F. R.; Lemcoff, N. O.; Semanscin, J. *Microporous Mesoporous Mater.* **2002**, *55*, 217.

(27) Myers, A. L.; Prausnitz, J. M. *AIChE J.* **1965**, *11*, 121.